21 April 2010 Volume 132 Number 15

THE JOURNAL OF CHEMICAL PHYSICS

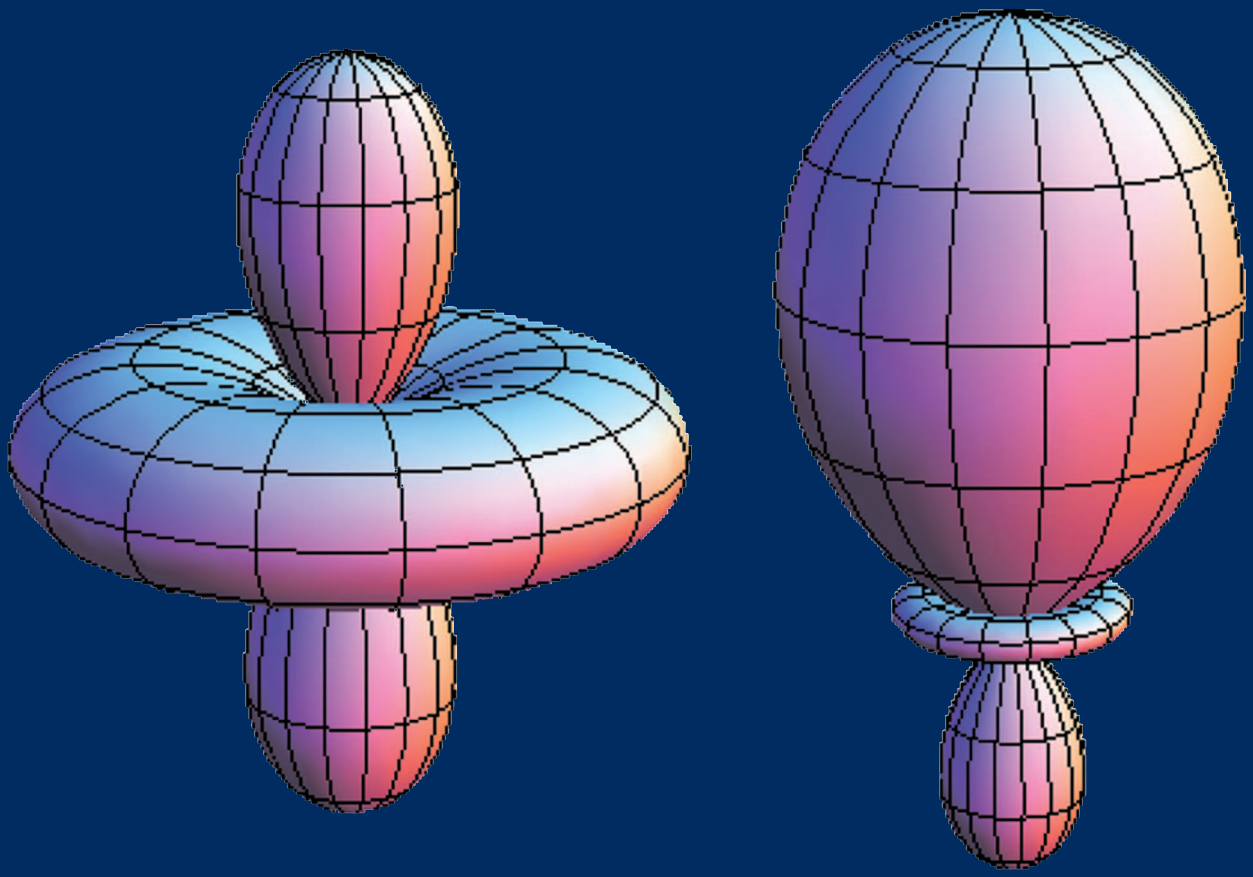

AIP

Preparation of polarized molecules using coherent infrared multicolor ladder excitation

Nandini Mukherjee and Richard N. Zare[a)]
Department of Chemistry, Stanford University, Stanford, California 94305-5080, USA

(Received 18 December 2009; accepted 9 February 2010; published online 15 April 2010)

A density matrix treatment is presented for a general process of preparing polarized molecules through their coherent interaction with two or more infrared photons of different frequencies, each tuned to cause a transition between real levels. This process, which might be called infrared stimulated Raman adiabatic passage, allows complete population transfer to selected rotational-vibrational levels and controls the direction of the rotational angular momentum vector $\boldsymbol{J}$ of the molecule with the possibility of preparing higher moments of the $\boldsymbol{J}$ spatial distribution. HCl molecules in a supersonic molecular beam are considered as a candidate system. Theory predicts that under collision-free conditions two infrared laser pulses of microsecond duration and milliwatt power are able to achieve complete population transfer and alignment of HCl ($v=2$, $J=2$, and $M=0$) for mutually parallel excitation and HCl ($v=2$, $J=2$, and $M=\pm 1$) for mutually perpendicular excitation. Orientation of the HCl ($v=2$, $J=2$, and $M=\pm 2$) can also be achieved using two circularly polarized pulses of the same helicity. For simplicity, our treatment ignores nuclear spin depolarization, which would be the case for molecules such as $^{12}C^{16}O$ and $^{12}C^{16}OO_2$. Polarized molecules in higher vibrational levels can be prepared using additional infrared pulses. © *2010 American Institute of Physics*. [doi:10.1063/1.3352553]

I. INTRODUCTION

Collisions between molecules and between atoms and molecules are usually studied with unpolarized targets, that is, the angular momentum vector of each reagent being randomly directed in space. Unfortunately, this approach averages over all possible M states and fails to give a clear picture of the stereochemistry of the collision process, whether it leads to reaction or to energy transfer. Consequently, many efforts have been made to prepare molecules so that they are aligned or oriented with respect to whatever target they collide with. For a comprehensive review see Ref. 1. It is important to define carefully what is meant by polarization preparation. An aligned molecular sample has the direction of its rotational angular momentum vector $\boldsymbol{J}$ such that the $|M|$ values of its projection on some quantization axis is unequally populated; an oriented molecular sample has unequal populations in $+M$ and $-M$ sublevels. We describe a general method for creating aligned or oriented molecules using coherent infrared excitation with cw laser sources. Several advantages exist for this procedure, including complete population transfer to the upper vibrational level, full control of the M sublevel distribution, and the need for laser sources of rather modest power and duration.

Optical Stark shift, which depends on the angle between the laser polarization and molecular axis, has been exploited to align molecules in ground vibrational levels.[2–4] The adiabatic alignment has been achieved in the presence of intense ($\sim 10^{12}$ W/cm^2) nanosecond pulses trapping the molecule in an angularly confined pendular state.[5,6] This technique however cannot generate the field-free alignment desired in a reactive collision. In the case of impulsive alignment a time-dependent superposition of rotational states is created using intense ($10^{13}-10^{14}$ W/cm^2) ultrashort pulses of $\sim 50-100$ fs duration.[7,8] The coherent superposition of a large number of rotational states creates a spatial confinement for the molecular axis which does not dissipate even after the optical pulse is gone. The field-free alignment shows periodic revivals with a period of a few picoseconds determined by the beat frequency of the rotational states. In each revival the alignment exists only for a short temporal window of less than a picosecond duration. The technique is attractive for probing various transient photochemical processes and has been applied to reconstruct the tomographic images of molecular orbitals using tunnel ionization during rephasing of the rotational wavepacket.[9] However, the low duty cycle and complicated synchronization scheme for impulsive alignment makes it not suitable for applications in the study of bimolecular reactions. Moreover, for studying reactive collisions, we are more interested in aligning molecules in excited vibrational levels having well-defined rotational levels.

For this purpose many techniques have been developed including stimulated Raman pumping,[10] chirped adiabatic Raman passage,[11] and stimulated Raman adiabatic passage (STIRAP).[12–14] In these examples the orientation-dependent multiphoton transition and $\Delta M=0$ and ± 1 selection rules for dipole-allowed transitions are exploited to create alignment and orientation for the excited molecule. However, most of these techniques generally require good control of the temporal and spectral shapes of the laser pulses and demand substantial optical power. Among these techniques, STIRAP

a)Electronic mail: zare@stanford.edu.

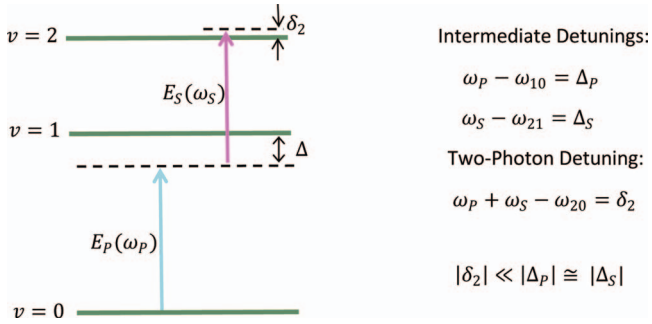

FIG. 1. Model nondegenerate three-level system where the vibrational levels are denoted by $v=0$, 1, and 2.

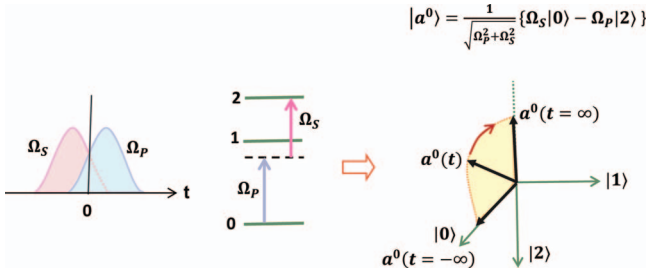

FIG. 2. Adiabatic evolution of the molecular eigenstate $|a^0(t)\rangle$ under counterintuitive excitation with Ω_P following Ω_S. In the beginning of the interaction, in the presence of Ω_S the molecular state is $|a^0(0)\rangle \equiv |0\rangle$. In the presence of both fields, $|a^0(t)\rangle$ evolves as a superposition of the bare states $|0\rangle$ and $|2\rangle$. At the end of the interaction $|a^0(t=+\infty)\rangle = -|2\rangle$.

has been demonstrated to be most efficient in transferring population to higher vibrational levels, and it demands the least amount of control on the laser pulse shapes and energy. Because the STIRAP process relies on near resonant coupling with the intermediate excited electronic states of the molecule, the wavelength often lies in the UV or vacuum ultraviolet (VUV) part of the spectrum. For the applications in reactive collisions involving variety of molecules, the preparation and use of tunable coherent VUV sources could be challenging and problematic. In addition, the loss of phase memory caused by the short lifetime of the intermediate electronic state generally demands appreciable intensity ($>\mathrm{W/mm^2}$) (Refs. 12–14) to achieve successful population transfer to the target vibrational level. In an effort to use relatively low power tunable laser sources, here we consider vibrational ladder climbing using the concept of adiabatic passage with delayed infrared pulses. As opposed to STIRAP involving electronically excited states, in an adiabatic climbing of a pure vibrational ladder the phase memory associated with the intermediate states is considerably longer. It will be shown here that the longer coherence time makes it possible to use a smaller Rabi frequency to satisfy the adiabatic condition and obtain complete population transfer to the final vibrational level. The required Rabi frequency may be available from the low power narrow-linewidth quantum cascade lasers (QCLs). We also consider a degenerate system where multiple adiabatic channels are coherently coupled by a combination of σ and π polarization of the exciting pulse sequence. In such a coupled system, a strong Zeeman coherence in the final vibrational level breaks the cylindrical symmetry and generates a higher-order spatial confinement for the rotational angular momentum. Similar adiabatic passage in degenerate quantum systems and the phase control of the final superposition state has been studied by Vewinger *et al.*[15,16] They have used Schrödinger equations to describe the ideal adiabatic transition in the absence of phase decay. To create molecular alignment using the phase coherent processes in a more robust environment, here we employ the density matrix formalism for a more comprehensive description of the dynamics and possible dephasing of the induced coherences. In what follows we briefly discuss the central idea of coherent ladder excitation via infrared STIRAP (IR STIRAP).

Figure 1 presents a three-level model vibrational system for coherent excitation. The Hamiltonian describing the laser-molecule interaction in the rotating wave approximation is given by

$$H = -\hbar \begin{pmatrix} 0 & \Omega_P & 0 \\ \Omega_P^* & \Delta_P & \Omega_S \\ 0 & \Omega_S^* & \Delta_P + \Delta_S \end{pmatrix} \tag{1}$$

where $\Omega_P = \mu_P E_P/\hbar$ and $\Omega_S = \mu_S E_S/\hbar$ are the Rabi frequencies associated with the $0 \rightarrow 1$ and $1 \rightarrow 2$ transitions, respectively. E_P and E_S are the slowly varying amplitudes of the optical fields at frequencies $\omega_P (\approx \omega_{10})$ and $\omega_S (\approx \omega_{21})$. They are expressed as $\vec{E}_P = \hat{z} E_P e^{i\omega_P t} + c.c.$ and $\vec{E}_S = \hat{z} E_S e^{i\omega_S t} + c.c.$ It is assumed that E_P resonantly couples the $0 \rightarrow 1$ transition with a detuning Δ_P, while E_S exclusively couples the $1 \rightarrow 2$ transition with a corresponding detuning Δ_S. For the case of ideal adiabatic passage in presence of a two-photon resonance ($\delta_2 \approx 0$ or $\Delta_P + \Delta_S \approx 0$), there exists a time-dependent eigenstate [similar to a trapped state or a dark state in electromagnetically induced transparency (EIT) (Refs. 12–14 and 17)] of the Hamiltonian in Eq. (1), which is a superposition of the initial and final vibrational levels (the bare states in absence of optical fields) given by

$$|a_0\rangle = \cos\Theta |0\rangle - \sin\Theta |2\rangle \tag{2}$$

where

$$\cos\Theta = \Omega_S / \sqrt{\Omega_P^2 + \Omega_S^2}$$

and

$$\sin\Theta = \Omega_P / \sqrt{\Omega_P^2 + \Omega_S^2}. \tag{3}$$

If the molecule is initially prepared in the eigenstate described in Eq. (2), using resonance excitation with a pair of time delayed pulses it will be trapped and evolve adiabatically remaining always in the eigenstate of the time-dependent Hamiltonian. For example, if Ω_S appears before Ω_P, such that at an earlier time we have $\cos\Theta = 1$ and $\sin\Theta = 0$, the molecule is entered into the trapped state $|a^0\rangle$ and continues to evolve, transforming smoothly into the bare state $|2\rangle$ at a later time when $\cos\Theta \rightarrow 0$ and $\sin\Theta \rightarrow 1$. In the Hilbert space, the time evolution corresponds to a smooth rotation of the molecular state $|a^0\rangle$ being parallel to the bare state $|0\rangle$ at earlier time and finally aligning along $|2\rangle$ with a phase shift of π at a later time, as shown in Fig. 2. The

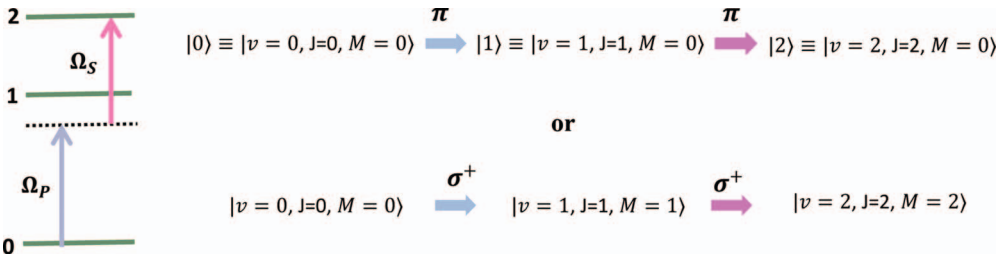

FIG. 3. A three-level system connected by two π or σ polarized photons. The two-step excitation from the ground vibrational level $v=0$ to the excited vibrational level $v=2$ via the $v=1$ intermediate level is carried out by a pair of resonant time-delayed pulse sequences. When the pump photons are both σ^+ or σ^- polarized, an orientation is created for the angular momentum $\boldsymbol{J}$ along the propagation direction of the laser beam.

remaining two other eigenstates of the 3×3 time-dependent Hamiltonian (not shown in Fig. 2) remain orthogonal to $|a^0\rangle$. The climbing of a ladder in the intuitive sense means that the system is first excited from the lowest level to the intermediate level followed by excitation from the intermediate level to the final level. As explained above, in a counterintuitive excitation sequence efficient ladder climbing occurs without losing population in the intermediate levels.

Using delayed pulse excitation in a counterintuitive sense, we show here that in addition to efficiently climbing the vibrational ladder, the adiabatic evolution creates angular momentum polarization by inducing Zeeman coherence among the magnetic sublevels of the excited rotational state. For the efficient population transfer to the excited vibrational level, the molecular state must remain trapped in the eigenstate $|a^0\rangle$ at all times without mixing with the other eigenstates ($|a^{\pm}\rangle$) of the time-dependent Hamiltonian. The smooth adiabatic evolution of the molecular eigenstate is ensured by the adiabatic following condition, which in the simplest form[12] is given by $\Omega\tau\gg1$ where τ is the interaction time. Thus, with increasing interaction time we may expect to achieve complete population transfer with cw optical power and relatively weak vibrational transition dipole moments. For the application to the supersonically expanded molecular beam, the interaction time τ is limited either by the transit time of the molecule through the beam waist or by the finite bandwidth of the exciting laser sources. In the following we show that using a laser linewidth of ~10 kHz and an interaction time of ~1 μs it is possible to achieve appreciable population transfer and alignment with relatively small cw laser power in the range of few tens of milliwatts.

II. THEORY

To demonstrate the idea, in the following we consider excitation of three- and four-level systems shown in Figs. 3 and 4, respectively. We calculate the population transfer and molecular alignment in the final vibrational level for various laser powers and detunings. For the convenience of describing Zeeman coherence and various damping processes, the density matrix equations are used to express the temporal dynamics.

A. Efficient population transfer in a three-level ladder system

The density matrix equations describing the optical excitation of a three-level ladder system in Fig. 1 or 3 are given below:

$$\frac{d\sigma_{01}}{dt} = -i\Delta_P\sigma_{01} + i\Omega_P(\rho_{11}-\rho_{00}) - i\sigma_{02}\Omega_S^*, \tag{4}$$

$$\frac{d\sigma_{12}}{dt} = -i\Delta_S\sigma_{12} + i\Omega_S(\rho_{22}-\rho_{11}) + i\sigma_{02}\Omega_P^*, \tag{5}$$

$$\frac{d\sigma_{02}}{dt} = -i\delta_2\sigma_{02} + i\Omega_P\sigma_{12} - i\sigma_{01}\Omega_S, \tag{6}$$

$$\frac{d\rho_{00}}{dt} = 2\,\mathrm{Re}\{i\Omega_P\sigma_{10}\}, \tag{7}$$

$$\frac{d\rho_{11}}{dt} = 2\,\mathrm{Re}\{i(\Omega_S\sigma_{21} + \Omega_P^*\sigma_{01})\}, \tag{8}$$

$$\frac{d\rho_{22}}{dt} = 2\,\mathrm{Re}\{i\Omega_S^*\sigma_{12}\}. \tag{9}$$

In Eqs. (4)–(9), the diagonal elements of the density matrix ρ_{00}, ρ_{11}, and ρ_{22} are proportional to the populations of the rovibrational levels $v=0$, $v=1$, and $v=2$, respectively.

σ_{ij} (for $i\neq j$) are the slowly varying Fourier amplitudes of the off-diagonal density matrix elements ρ_{ij} defined by[18,19] $\rho_{ij}=\sigma_{ij}(\omega)e^{i\omega t}+\sigma_{ij}(-\omega)e^{-i\omega t}$, where ω is the frequency of the optically driven coherence for the superposition of the ith

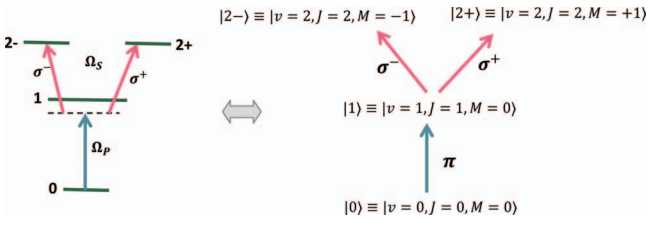

FIG. 4. A four-level molecular system connected by two photons with orthogonal polarizations. Levels $2-$ and $2+$ represent the degenerate rotational sublevels $M=-1$ and $M=+1$ of the upper excited state ($v=2$, $J=2$). The quantization axis for the angular momentum is chosen along the direction of the linearly polarized coupling field Ω_P. The second photon is a superposition of two states with opposite circular polarizations. The second photon thus coherently couples the two magnetic sublevels, $2-$ and $2+$, and creates a higher-order $\boldsymbol{J}$ spatial anisotropy, as discussed in the text.

TABLE I. Parameter for HCl in coherent ladder climbing.

Laser line-width	δ_2	Δ_P, Δ_S	Pulse length τ_P	Ω (10^6 rad/s)	μ_v HCl $v=0\rightarrow v=1$	μ_v HCl $v=1\rightarrow v=2$
~10 kHZ	≥2× laser linewidth	~100 kHZ	~1 μs for ~1 mm Gaussian beam waist	~4 for laser intensity 30–40 mW/mm^2	0.072 D [estimated using HITRAN (Ref. 20)]	~0.099 D [estimated using HITRAN (Ref. 20)]

and jth molecular quantum states. In this example we are interested in the resonant frequency components $\sigma_{01}(\omega_P)$, $\sigma_{12}(\omega_S)$, and $\sigma_{02}(\omega_P+\omega_S)$. The complex detunings associated with the $0\rightarrow1$ and $1\rightarrow2$ transitions are given by $\Delta_P=\omega_P-\omega_{10}-i\gamma_{01}$ and $\Delta_S=\omega_S-\omega_{21}-i\gamma_{12}$. The two-photon detuning $\delta_2=(\omega_P+\omega_S)-\omega_{20}-i\gamma_{02}$.

γ_{ij} represents the dephasing rate for the molecular coherence σ_{ij}. In the absence of radiative and collisional damping (as in the case of a supersonic beam), γ_{ij} can be used to model the phase fluctuations of the laser fields as described in the following section. The radiative damping from the excited vibrational levels is neglected. The optical fields and the Rabi frequencies $\vec{\Omega}_P$ and $\vec{\Omega}_S$ in the above equations are assumed to be either linearly polarized parallel to the z-axis or circularly polarized with identical helicities. With two identical linearly polarized laser fields the population is transferred from the initial level ($v=0$, $J=0$, and $M=0$) to the final level ($v=2$, $J=2$, and $M=0$) creating an alignment for the excited molecule. As shown in Fig. 3, with two right circularly polarized optical fields, the population is transferred from initial ($v=0$, $J=0$, and $M=0$) level to the final ($v=2$, $J=2$, and $M=2$) level. This excitation creates an orientation and alignment for the angular momentum of the excited molecule along the propagation direction of the optical beam. Equations (4)–(9) are solved numerically for the excitation of the $v=2$ level of HCl for various detunings of the intermediate $v=1$ level, assuming here and throughout that for simplicity we can ignore nuclear spin. For the collision-free ambience of a supersonic molecular beam we assume $\gamma_{01}=\gamma_{12}=\gamma_{02}=0$ for an interaction time of ~1 or 2 μs. We consider the case of a small but finite detuning for the two-photon resonance $\delta_2=\Delta_P+\Delta_S\approx2\times$ laser linewidth. This approach is consistent with the finite bandwidth of the exciting lasers leading to phase fluctuations and limiting us from reaching the $\delta_2=0$ condition. The parameters used in the numerical calculations are listed in Table I.

Figure 5 shows the result of a numerical calculation using a laser linewidth of 10 kHz, a two-photon detuning of 20 kHz, and pulse duration of 1 μs. A Gaussian optical field of the form $E(t)=e^{-(t/\tau_P)^2}$ is assumed. The pulse length τ_P is determined by the transit time through the laser beam, i.e., $\tau_P=w/v$, where w is the beam waist and v (~1000 m/s) is the supersonic speed of the molecule. It should be noted that a much narrower laser linewidth compared to the apparent transit time broadening is used here to avoid dephasing during the prolonged interaction with a Gaussian optical pulse having an exponential tail. Figure 5 shows that in presence of a nonzero δ_2, and intermediate level detunings of $\Delta_P/2\pi\approx\Delta_S/2\pi\approx100$ kHz, 99% of the population can be transferred using the counterintuitive pulse sequence with Rabi frequency $\Omega_P\approx\Omega_S\approx3.8\times10^6$ rad/s. The optimum delay between the pulses is found to be ~1 μs. This example marginally satisfies the adiabatic following condition with $\Omega\tau\approx3.8$. As mentioned earlier, with a proper choice of polarizations for the optical fields, we create orientation and alignment for the vibrationally excited molecule. The angular momentum polarization in the $v=2$ level is calculated using the orientation and alignment parameters defined by[21,22]

$$A_q^{(k)}=\frac{c(k)}{\langle JM|J^2|JM\rangle^{k/2}}\langle J_q^{(k)}\rangle, \tag{10}$$

where $\langle J_q^{(k)}\rangle=\Sigma_{MM'}\rho_{MM'}^J\langle JM|J_q^{(k)}|JM'\rangle$ and $J_q^{(k)}$ are spherical tensor operators of order k and rank q. For the excitation with two circularly polarized photons with identical helicity, there is cylindrical symmetry about the propagation direction of the optical beam. The cylindrical symmetry also persists in case of two linearly polarized photons parallel to the z-axis. In the presence of cylindrical symmetry, only the $q=0$ terms exist for $A_q^{(k)}$, and the angular momentum polarization is described by a classical probability density

$$\rho(\theta,\phi)=\frac{1}{4\pi}\left[1+3A_0^{(1)}\cos(\theta)+\frac{5}{2}A_0^{(2)}(3\cos^2(\theta)-1)+\cdots\right] \tag{11}$$

Figures 6(a) and 6(b) illustrate the three-dimensional polar plots of $\rho(\theta,\phi)$ calculated for the excitation with linearly and circularly polarized laser fields.

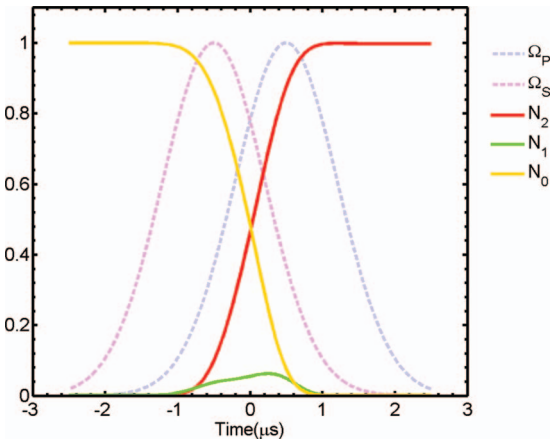

FIG. 5. The temporal dynamics of population transfer to the two-photon resonant vibrational level (level $v=2$ in Fig. 1) using 2π polarized infrared photons. N_0, N_1, and N_2 represent the fractional populations in the vibrational levels $v=0$, $v=1$, and $v=2$ of the HCl molecule equivalent to a three-level system discussed in Figs. 1–3. The parameters for the calculation are: $\delta_2/2\pi=20$ kHz, $\Delta_P/2\pi=100$ kHz, $\tau_P=1$ μs, $\tau_D=\tau_P$, and $\Omega_P=\Omega_S=3.8\times10^6$ rad/s. Complete population transfer is achieved when Ω_S arrives earlier than Ω_P and dresses up the molecule for the adiabatic interaction.

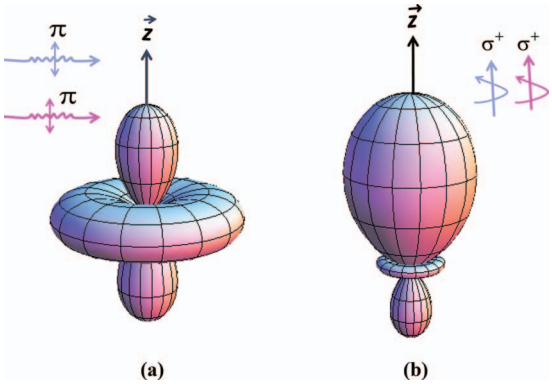

FIG. 6. Angular momentum polarization in the rovibrational level $v=2$, $J=2$ with (a) two π polarized photons parallel to the quantization z axis and (b) with two σ^+ polarized photons propagating along the z axis. In (a) the orientation and alignment parameters are: $A_0^{(1)}=0$ and $A_0^{(2)}=-1$. In (b) they are $A_0^{(1)}=0.82$ and $A_0^{(2)}=1$.

In the following we discuss the terms and conditions for optimizing the population transfer and alignment using delayed pulse excitation. In Fig. 7 population transfer versus laser intensity is plotted for different values of two-photon detunings. We find that substantially higher power is required when the two-photon detuning becomes comparable to the Rabi frequency (~0.6 MHz). Using a similar calculation it can be shown that the efficiency of an adiabatic transfer is much less sensitive to the intermediate level detunings. In Fig. 8 we have plotted the transfer efficiency versus pulse delay with a positive delay implying the counterintuitive sequence. It is interesting to note that even in presence of finite two-photon detuning and a weak adiabatic condition, the counterintuitive sense of excitation is able to trap the molecule in the eigenstate defined in Eq. (2). The significance of counterintuitive excitation is exemplified in Fig. 9, where we have plotted the population transfer as a function of Rabi frequency for the pulse delays $\tau_D=0$, 1, and -1 μs. Figure 9 shows that the Rabi oscillations dominate the population

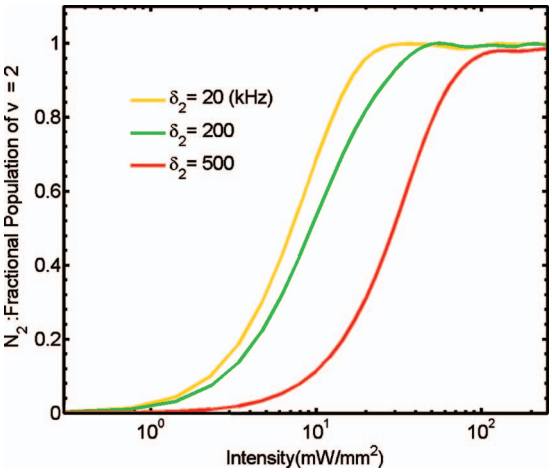

FIG. 7. Fractional population transferred to $v=2$, $J=2$ rovibrational level as a function of the pump intensity for three values of the two-photon detuning $\delta_2/2\pi=20$, 200, and 500 kHz. Efficient adiabatic population transfer occurs with minimum laser intensity in presence of an ideal condition of two-photon resonance. The single photon detuning and pulse duration used in the calculation are: $\Delta_P/2\pi=100$ kHz and $\tau_P=1$ μs. Calculated intensity is shown for the π polarized optical fields.

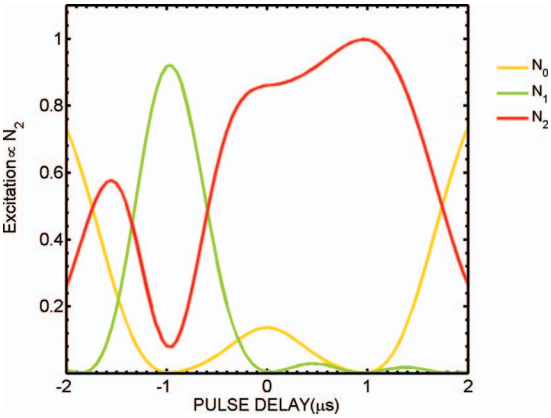

FIG. 8. Population transferred to the $v=2$, $J=2$ rovibrational level of HCl as a function of delay between the two laser pulses Ω_S and Ω_P. Here, positive delay means counterintuitive excitation where Ω_S appears before Ω_P. Maximum population transfer occurs for positive delay $\cong 1$ μs. The parameters used in the calculation are: $\delta_2/2\pi=20$ kHz, $\Delta_P/2\pi=100$ kHz, $\tau_P=1$ μs, and $\Omega_P=\Omega_S=3.8\times10^6$ rad/s.

transfer for the negative and zero delay. With the Rabi frequency $\Omega\approx4\times10^6$ rad/s, stable and consistent population transfer is seen to occur only for $\tau_D=+1$ μs requiring the early arrival of Ω_S and a delayed interaction with Ω_P. For the above calculations, we neglected the decay of coherence during the interaction time of $1-2$ μs. As pointed out before, the transfer efficiency may be limited by the phase fluctuations of the optical fields of finite bandwidth. The phase fluctuations can be modeled using equivalent damping rate for the molecular coherence. Figure 10 shows that because of the loss of phase memory, the transfer efficiency is limited to a lower value even after using higher optical power. Kuhn *et al.*[23] have studied the adiabatic population transfer using spectrally broad light. Their study indicated a high sensitivity of transfer efficiency on the autocorrelation of the fluctuating light.

The above theoretical analysis suggests that using moderate laser intensity of a few tens of milliwatts, sufficient excitation and alignment is possible even when the two-

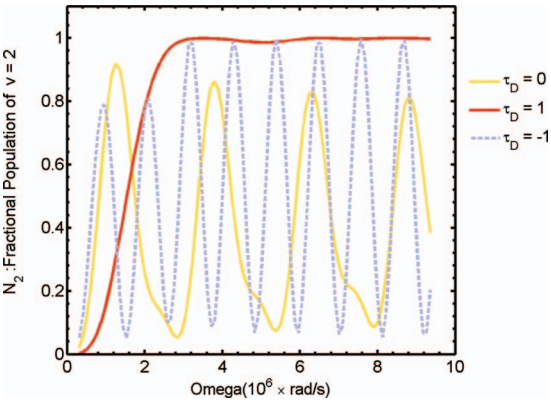

FIG. 9. Population transferred to rovibrational level $v=2$, $J=2$ vs Rabi frequency for three different pulse delays: $\tau_D=0$, 1, and -1 μs. The other parameters for the calculations are: $\delta_2/2\pi=20$ kHz, $\Delta_P/2\pi=100$ kHz, and $\tau_P=1$ μs. The positive delay implies counterintuitive excitation where Ω_S appears before Ω_P. For a positive delay, $\tau_D=1$ μs, complete population transfer occurs for Rabi frequencies $\Omega_P=\Omega_S\geq3.2\times10^6$ rad/s. The population transfer fluctuates as a function of pulse area for $\tau_D=0$ and -1 μs.

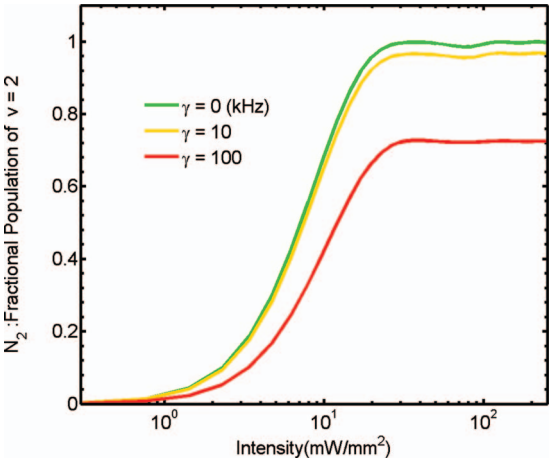

FIG. 10. Population transferred to rovibrational level $v=2$, $J=2$ as a function of laser pulse intensity in presence of phase fluctuation. The phase fluctuation of the optical field is modeled using the decoherence rates γ for the off-diagonal density matrix elements. Significant damping of phase coherence limits the achievable population transfer as seen in the case of $\gamma/2\pi=100$ kHz The other parameters for calculation are the same as in Fig. 5.

photon resonance is not perfect and adiabatic condition is only weakly satisfied. Because the procedure relies on the preparation of a molecular eigenstate using coherent optical interaction, the efficiency is affected strongly by the phase fluctuations of the laser field. A practical application of the technique would therefore call for the laser phase and frequency stabilization to be within a linewidth of ~10 kHz. It is also possible to effectively remove the phase decoherence by reducing the interaction time with an optical field having a wider linewidth (~100 kHz). Because the laser intensity $I \propto \Omega^2$ and the adiabatic following condition requires $\Omega \propto 1/\tau$, shortening the interaction time generally requires higher pump intensity. However, we should note that in the case of a supersonic molecular beam, $\tau \propto w$ (the beam waist) and therefore decreasing τ does not require higher laser power which is proportional to Iw^2. The Rabi frequency used in the example of Fig. 5 can be reached with a laser intensity of 30–40 mW/mm^2 which is well within the range of a single-mode QCL.[24–27]

B. Excitation to higher vibrational levels with higher-order polarization in a four-level system

Next we consider the Zeeman coherence and molecular alignment in the vibrational level using parallel and perpendicular delayed pulse excitation, as shown in Fig. 4. The linearly polarized optical fields are given by

$$\vec{E}_P(\omega_P) = \hat{z}E_P e^{i\omega_P t} + c.c.,$$

$$\vec{E}_S(\omega_S) = \hat{x}E_S e^{i\omega_S t} + c.c. = \frac{1}{\sqrt{2}}(\hat{e}_+ + \hat{e}_-)E_S e^{i\omega_S t} + c.c. \quad (12)$$

The pump field $\vec{E}_P(\omega_P)$ is polarized along the molecular quantization $\hat{z}$ axis and resonantly couples $|v=0,J=0,M=0\rangle$ with the $|v=1,J=1,M=0\rangle$ level. The pump field $\hat{x}E_S(\omega_S)$ can be written as a superposition of right and left circularly polarized component waves. The right and left circularly polarized optical fields couple the intermediate level $|v=1,J=1,M=0\rangle$ with the upper quantum levels $|v=2,J=2,M=\pm 1\rangle$ as shown in Fig. 4. In addition, the nonlinear optical interaction induces Raman coherence among the magnetic sublevels $M=\pm 1$ of the $(v=2, J=2)$ level.

The density matrix equations describing the four-level system are given below:

$$\frac{d\sigma_{01}}{dt} = -i\Delta_{01}\sigma_{01} + i\Omega_P(\rho_{11}-\rho_{00}) - i\frac{\Omega_S^*}{\sqrt{2}}(\sigma_{02-}-\sigma_{02+}), \quad (13)$$

$$\frac{d\sigma_{12+}}{dt} = -i\Delta_{12}\sigma_{12+} - i\frac{\Omega_S}{\sqrt{2}}(\rho_{2+2+}-\rho_{11}) + i\Omega_P^*\sigma_{02+} + i\frac{\Omega_S}{\sqrt{2}}\sigma_{2-2+}, \quad (14)$$

$$\frac{d\sigma_{12-}}{dt} = -i\Delta_{12}\sigma_{12-} + i\frac{\Omega_S}{\sqrt{2}}(\rho_{2-2-}-\rho_{11}) + i\Omega_P^*\sigma_{02-} - i\frac{\Omega_S}{\sqrt{2}}\sigma_{2+2-}, \quad (15)$$

$$\frac{d\sigma_{02-}}{dt} = -i\delta_2\sigma_{02-} + i\Omega_P\sigma_{12-} - i\frac{\Omega_S}{\sqrt{2}}\sigma_{01}, \quad (16)$$

$$\frac{d\sigma_{02+}}{dt} = -i\delta_2\sigma_{02+} + i\Omega_P\sigma_{12+} + i\frac{\Omega_S}{\sqrt{2}}\sigma_{01}, \quad (17)$$

$$\frac{d\sigma_{2-2+}}{dt} = -i\Delta_{2-2+}\sigma_{2-2+} + i\frac{\Omega_S^*}{\sqrt{2}}\sigma_{12+} + i\frac{\Omega_S}{\sqrt{2}}\sigma_{2-1}, \quad (18)$$

$$\frac{d\rho_{00}}{dt} = 2\,\mathrm{Re}\{i\Omega_P\sigma_{10}\}, \quad (19)$$

$$\frac{d\rho_{11}}{dt} = 2\,\mathrm{Re}\left\{i\Omega_P^*\sigma_{01} + i\frac{\Omega_S}{\sqrt{2}}(\sigma_{2-1}-\sigma_{2+1})\right\}, \quad (20)$$

$$\frac{d\rho_{2-2-}}{dt} = 2\,\mathrm{Re}\left\{i\frac{\Omega_S^*}{\sqrt{2}}\sigma_{12-}\right\}, \quad (21)$$

$$\frac{d\rho_{2+2+}}{dt} = -2\,\mathrm{Re}\left\{i\frac{\Omega_S^*}{\sqrt{2}}\sigma_{12+}\right\}, \quad (22)$$

In Eqs. (13)–(22) "2+" and "2−" represent the magnetic sublevels $M=+1$ and $M=-1$ of the $(v=2, J=2)$ level, respectively, as shown in Fig. 4. σ_{2-2+} represents the Zeeman coherence while ρ_{2+2+} and ρ_{2-2-} represent the populations of the magnetic sublevels $M=+1$ and $M=-1$ belonging to the upper rovibrational level $v=2$, $J=2$.

The relevant detunings are given by:

$$\Delta_{01} = \omega_P - \omega_{10} - i\gamma_{01},$$

$$\Delta_{12} = \omega_S - \omega_{21} - i\gamma_{12},$$

$$\delta_2 = (\omega_P + \omega_S) - \omega_{20} - i\gamma_{02},$$

$$\Delta_{2-2+} = -i\Gamma_{2-2+},$$

where Γ_{2-2+} is the dephasing rate for the Zeeman coherence σ_{2-2+} and is also the depolarization rate for the target rovibrational level $v=2$, $J=2$.

For the four-level system described by the set of Eqs. (13)–(22) the population in the final $v=2$ vibrational level is given by $N_2 \propto (\rho_{2-2-}+\rho_{2+2+})$. Equations (13)–(22) describe the dynamics of two coherently coupled adiabatic processes $(0\rightarrow 1\rightarrow 2-)$ and $(0\rightarrow 1\rightarrow 2+)$. The coupling is accomplished by the Raman interaction between the two sublevels ($v=2$, $J=2$, and $M=-1$) and ($v=2$, $J=2$, and $M=+1$) via the common intermediate level ($v=1$, $J=1$, and $M=0$). As a result of the coupled interactions a sizable Zeeman coherence σ_{2-2+} is created in the final $v=2$ vibrational level. The Zeeman coherence breaks the cylindrical symmetry and creates nonzero components for the second-order spherical tensor operator $J_q^{(2)}$. We calculate the angular momentum polarization in the $v=2$ state using the orientation and alignment parameters defined in Eq. (10). From the symmetry of the optical interactions shown in Fig. 4, the orientation parameter is $A_{0,\pm 1}^{(1)}=0$. The various components of the alignment parameter proportional to the quadrupolar moments of $\boldsymbol{J}$ are given below

$$A_q^{(2)}(J) = \frac{\sqrt{6}}{J(J+1)}\langle J_q^{(2)}\rangle, \tag{23}$$

where $q=0$, ± 1, and ± 2.

From the symmetry consideration

$$\langle J_{\pm 1}^{(2)}\rangle = 0, \tag{24}$$

$$\langle J_0^{(2)}\rangle = \frac{1}{\sqrt{6}}\sum_M \rho_{MM}[3M^2 - J(J+1)], \tag{25}$$

$$\begin{aligned}\langle J_{+2}^{(2)}\rangle &= \frac{1}{2}\langle J_+^2\rangle \\ &= \frac{1}{2}\sum_{MM'} \rho_{MM'}^J \langle JM|J_+^2|JM'\rangle \\ &= \frac{1}{2}\sum_M \rho_{MM-2}^J [\sqrt{J(J+1)-(M-2)(M-1)} \\ &\quad \times \sqrt{J(J+1)-M(M-1)}],\end{aligned} \tag{26}$$

where we have used the property of the raising operator $\hat{J}_+ = \hat{J}_x + i\hat{J}_y$ in the last equality in Eq. (26). ρ_{MM-2}^J represents the Zeeman coherence among the rotational sublevels (JM) and $(JM-2)$. Using Eqs. (23)–(26) we calculate the alignment parameters for the rotational angular momentum in the final rovibrational level $v=2$, $J=2$ of the four-level ladder system

$$A_0^{(2)}(J=2) = -\tfrac{1}{2}(\rho_{2-2-}+\rho_{2+2+}), \tag{27}$$

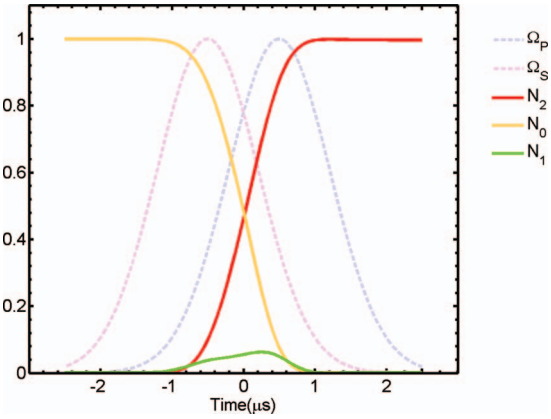

FIG. 11. Temporal dynamics of population transfer to the excited rovibrational $v=2,J=2$ level of the HCl molecule with parallel and perpendicular optical fields. The equivalent four-level molecular system is shown in Fig. 4. N_0 and N_1 represent the fractional populations in the vibrational $v=0$ and intermediate $v=1$ levels, respectively. $N_2=N_{2-}+N_{2+}$ is the total fractional population of the degenerate $v=2$, $J=2$ rovibrational level of the four-level molecular system. The laser pulses Ω_S and Ω_P are applied in a counterintuitive sense for efficient adiabatic transfer of population from the $(v=0,J=0)\rightarrow(v=2,J=2)$ rovibrational level. Parameters for calculation are: $\delta_2/2\pi=20$ kHz, $\Delta_P/2\pi=100$ kHz, $\tau_P=1$ μs, $\tau_D=\tau_P$, and $\Omega_P=\Omega_S=3.8\times 10^6$ rad/s.

$$A_{\pm 2}^{(2)}(J=2) = \sqrt{\frac{3}{2}}\sigma_{2-2+}. \tag{28}$$

Figures 11 and 12 show the temporal dynamics of the excited state population and Zeeman coherence for a pulse length of ~ 1 μs with $\Omega_P=\Omega_S=3.8\times 10^6$ rad/s. The optimum time delay between the pulses is again found to be ~ 1 μs. The calculated alignment parameters $A_0^{(2)}\cong -0.5$ and $A_{\pm 2}^{(2)}\cong -0.6$ can be used to describe an angular momentum polarization in the rovibrational level $v=2$, $J=2$ using the classical probability density as follows:

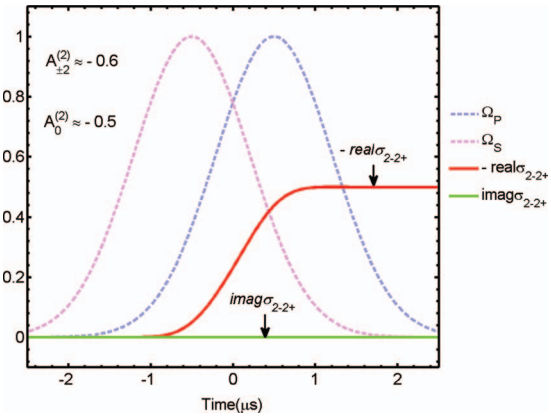

FIG. 12. The temporal evolution of the real and imaginary parts of the Zeeman coherence $\sigma_{2-2+}\equiv\langle v=2,J=2,M=-1|\hat{\rho}|v=2,J=2,M=+1\rangle$. σ_{2-2+} is induced during the interaction of two coherently coupled adiabatic passages. The excited state coherence breaks the cylindrical symmetry and creates higher-order alignment for the rotational angular momentum defined by the parameters $A_0^{(2)}\cong -0.5$ and $A_{\pm 2}^{(2)}\cong -0.6$. The parameters used for the calculation are the same as in Fig. 11.

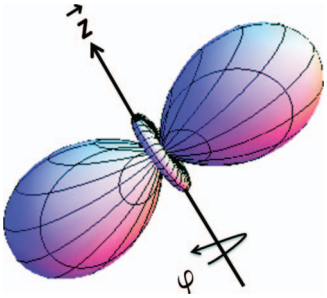

FIG. 13. The angular momentum polarization in the $v=2$, $J=2$ rovibrational level of the HCl molecule excited by a sequence of time-shifted resonant infrared pulses of microsecond duration. The cylindrical symmetry is broken by inducing coherence among the magnetic sublevels belonging to the $v=2$, $J=2$ rovibrational level. The z axis is oriented along the polarization of the optical pulse resonantly coupling the ground and intermediate vibrational levels. For the other pulse the electric filed is oriented perpendicular to the z axis.

$$\rho(\theta,\phi)=\frac{1}{4\pi}\left[1+\frac{5}{2}A_0^{(2)}(3\cos^2\theta-1)+5\sqrt{\frac{3}{2}}A_2^{(2)}\sin^2\theta\cos 2\phi\right], \tag{29}$$

where $\rho(\theta,\phi)$ is the probability density for locating the rotational angular momentum vector within a unit solid angle defined by the polar angle θ and azimuthal angle ϕ relative to the quantization (z) axis of the molecule. The symmetry with respect to the polar angle θ implies pure alignment in absence of orientation. Any ϕ dependence indicates absence of cylindrical symmetry caused by the induced Zeeman coherence. Figure 13 shows the angular momentum polarization achieved with parallel and perpendicular infrared pulses of ~ 40 mW/mm^2 intensity and 1 μs duration. With a relative angle of 45° between the linearly polarized pump fields, it is possible to break the spatial symmetry even further and induce alignment with a nonzero value for the moment of the spherical tensor $J_{\pm 1}^{(2)}$ or $A_{\pm 1}^{(2)}$.

C. Consideration for ideal infrared laser sources

It is possible to adiabatically transfer population to the higher vibrational level $v=4$ using sequential STIRAP with a 5-state molecular system and create alignment with high spatial order. The two most important criteria to achieve higher-order ladder excitation and polarizations are: (1) fulfill the adiabatic following condition and (2) eliminate phase decoherence during the prolonged interaction time with a sequence of delayed Gaussian pulses. The first condition is met, as we have shown above, with 1 μs long pulses and a Rabi frequency Ω satisfying $\Omega\tau\approx 4$. This requires a laser intensity of ~ 30 to 40 mW/mm^2. To meet the second condition the laser frequency must be stabilized to a frequency width of ~ 10 kHz. We note that single-mode QCLs are ideally suited for this purpose. Owing to a small linewidth enhancement factor of the QCL, the frequency stabilization can significantly reduce the laser linewidth.[28] For example, the laser frequency ω_P can be stabilized to the Lamb dip of the transition $(v=0,J=0,M=0)\rightarrow(v=1,J=1,M=0)$ using counterpropagating pump probe spectroscopy of HCl contained in a gas cell at low pressure of a few millitorrs. In the presence of the first pump locked to the resonance frequency ω_{10}, a second QCL at frequency ω_S can be tuned to the absorption peak of the $(v=1,J=1,M=0)\rightarrow(v=2,J=2,M=0)$ transition and stabilized to the Doppler-free absorption lineshape. Although, the resonant wavelengths for the two transitions of HCl molecule at 3.44 μm ($\omega_P\approx 2906$ cm^{-1}) and 3.54 μm ($\omega_S\approx 2820.72$ cm^{-1}) are sitting at the very edge of presently available QCLs, we may expect to meet the relatively low power requirement and frequency stability for the single-mode operation using a DFB or an external grating tuned cavity.

III. CONCLUSION

We have shown that significant alignment and orientation can be achieved in excited rovibrational levels of a molecule using coherent excitation of a rovibrational ladder with time separated infrared pulse sequences (IRSTIRAP). To take advantage of the "adiabatic passage" the pulses are applied in a counterintuitive sense of their sequence and the molecule is trapped in the desired adiabatic eigenstate of the optically dressed Hamiltonian. The optical interaction induces coherence among the magnetic sublevels of the final rovibrational excited state via two-photon Raman-type coupling. The induced Zeeman coherence breaks the cylindrical symmetry and creates higher moments for the angular momentum polarization of the excited molecule. The process we have described is the infrared analog of electronic STIRAP in the use of real rovibrational levels that are climbed as a ladder. We have applied this technique to a supersonic beam of HCl molecules as a test case. We show that efficient ladder climbing to the vibrational level $v=2$ with 100% population transfer can be achieved using low intensity infrared pulses of microsecond duration. The condition for the adiabatic evolution of the molecular quantum state can be fulfilled using narrow linewidth (~ 10 kHz) low power (~ 40 mW/mm^2) single-mode DFB or external cavity QCLs. The procedure can be applied to small infrared-active molecules whose vibrational structure is relatively uncongested. The adiabatic ladder excitation and alignment technique described here can be extended to efficiently transfer population to higher vibrational levels ($v=4,6$) using sequential STIRAP (Ref. 29) with partially overlapping pulses as long as the coherence is maintained during the interaction time. Adiabatic ladder excitation to ($v=3,5$), etc., is also possible by manipulating the intermediate level detunings and laser intensities.[30] QCLs can provide the optical fields at variety of wavelengths for a broad range of molecular resonance conditions. We suggest that coherent infrared multicolor ladder excitation opens the possibility of preparing energetically hot coherent sates of polarized molecules for studying the stereodynamics of chemical reactions.

ACKNOWLEDGMENTS

We thank Professor Klaas Bergmann for many helpful discussions. This work has been supported by the National Science Foundation under Grant No. NSF CHE 0650414.

[1] *Vector Correlation and Alignment in Chemistry*, edited by G. G. Balint-Kurti and M. P. de Miranda, [Collaborative Computational Project on Molecular Quantum Dynamics (CCP6), Warrington, United Kingdom, 2006]; http://www.ccp6.ac.uk/booklets/CCP6-2005_vector_correlations.pdf
[2] H. Stapelfeldt and T. Seideman, Rev. Mod. Phys. **75**, 543 (2003).
[3] T. Seideman, J. Chem. Phys. **103**, 7887 (1995).
[4] H. Sakai, C. P. Safvan, J. J. Larson, K. K. Hilligsøe, K. Hald, and H. Stapelfeldt, J. Chem. Phys. **110**, 10235 (1999).
[5] H. Stapelfeldt, Phys. Scr., T **110**, 132 (2004).
[6] L. Holmegaard, J. H. Nielsen, I. Nevo, H. Stapelfeldt, F. Filsinger, J. Kupper, and G. Meijer, Phys. Rev. Lett. **102**, 023001 (2009).
[7] F. Rosca Pruna and M. J. J. Vrakking, Phys. Rev. Lett. **87**, 153902 (2001).
[8] P. W. Dooley, I. Litvinyuk, K. F. Lee, D. M. Rayner, M. Spanner, D. M. Villeneuve, and P. B. Corkum, Phys. Rev. A **68**, 023406 (2003).
[9] J. Itatani, J. Levesque, D. Zeidler, H. Niikura, H. Pepin, J. C. Keiffer, P. B. Corkum, and D. M. Villeneuve, Nature (London) **432**, 867 (2004).
[10] N. C. M. Bartlett, D. J. Miller, R. N. Zare, D. Sofikitis, T. P. Rakitzis, and A. J. Alexander, J. Chem. Phys. **129**, 084312 (2008).
[11] F. Legare, S. Chelkowski, and A. D. Bandrauk, Chem. Phys. Lett. **329**, 469 (2000).
[12] N. V. Vitanov, M. Fleischhauer, B. W. Shore, and K. Bergmann, Adv. At., Mol., Opt. Phys. **46**, 55 (2001).
[13] K. Bergmann, H. Theuer, and B. W. Shore, Rev. Mod. Phys. **70**, 1003 (1998) and references therein.
[14] U. Gaubatz, P. Rudeck, S. Schiemann, and K. Bergmann, J. Chem. Phys. **92**, 5363 (1990).
[15] F. Vewinger, M. Heinz, B. W. Shore, and K. Bergmann, Phys. Rev. A **75**, 043406 (2007).
[16] F. Vewinger, M. Heinz, U. Schneider, C. Barthel, and K. Bergmann, Phys. Rev. A **75**, 043407 (2007).
[17] S. E. Harris, Phys. Rev. Lett. **70**, 552 (1993).
[18] N. Mukherjee, J. Opt. Soc. Am. B **23**, 1635 (2006).
[19] P. W. Milonni and J. H. Eberly, J. Chem. Phys. **68**, 1602 (1978).
[20] L. S. Rothmana, D. Jacquemarta, A. Barbeb, D. C. Bennerc, M. Birkd, L. R. Browne, M. R. Carleerf, C. Chackerian, Jr., K. Chancea, L. H. Coudert, V. Danai, V. M. Devic, J.-M. Flaudh, R. R. Gamachej, A. Goldmank, J.-M. Hartmannh, K. W. Jucksl, A. G. Makim, J.-Y. Mandini, S. T. Massien, J. Orphalh, A. Perrinh, C. P. Islands, M. A. H. Smitho, J. Tennysonp, R. N. Tolchenovp, R. A. Tothe, J. Vander Auweraf, P. Varanasiq, and G. Wagnerd, J. Quant. Spectrosc. Radiat. Transf. **96**, 139 (2005).
[21] A. J. Orr-Ewing and R. N. Zare, Annu. Rev. Phys. Chem. **45**, 315 (1994).
[22] R. N. Zare, *Angular Momentum: Understanding Spatial Aspects in Chemistry and Physics* (Wiley Interscience, NY, 1988).
[23] A. Kuhn, G. W. Coulston, G. Z. He, S. Schiemann, K. Bergmann, and W. S. Warren, J. Chem. Phys. **96**, 4215 (1992).
[24] G. Wysocki, R. F. Curl, F. K. Tittel, R. Maulini, J. M. Bulliard, and J. Faist, Appl. Phys. B: Lasers Opt. **81**, 769 (2005).
[25] N. Mukherjee and C. K. N. Patel, Chem. Phys. Lett. **462**, 10 (2008).
[26] R. Maulini, I. Dunayvskiy, A. Lyakh, A. Tsekoun, C. K. N. Patel, L. Diehl, C. Pflugl, and F. Capasso, Electron. Lett. **45**, 107 (2009).
[27] J. Devenson, O. Cathabard, R. Teissier, and A. N. Baranov, Appl. Phys. Lett. **91**, 141106 (2007).
[28] R. M. Williams, J. F. Kelly, J. S. Hartman, S. W. Sharpe, M. S. Taubman, J. L. Hall, F. Capasso, C. Gmachl, D. L. Sivco, J. N. Baillargeon, and A. Y. Cho, Opt. Lett. **24**, 1844 (1999).
[29] H. Theuer and K. Bergmaan, Eur. Phys. J. D **2**, 279 (1997).
[30] N. V. Vitanov, B. W. Shore, and K. Bergmaan, Eur. Phys. J. D **4**, 15 (1998).